biomolecules

MDPI

Article

Development of Improved Spectrophotometric Assays for Biocatalytic Silyl Ether Hydrolysis

Yuqing Lu [1,2,†], Chisom S. Egedeuzu [1,2,†], Peter G. Taylor [3] and Lu Shin Wong [1,2,*]

[1] Manchester Institute of Biotechnology, University of Manchester, Manchester M1 7DN, UK; yuqing.lu-3@postgrad.manchester.ac.uk (Y.L.); chisom.egedeuzu@manchester.ac.uk (C.S.E.)
[2] Department of Chemistry, University of Manchester, Manchester M13 9PL, UK
[3] School of Life Health and Chemical Sciences, Open University, Milton Keynes MK7 6AA, UK; peter.taylor@open.ac.uk
* Correspondence: l.s.wong@manchester.ac.uk
† These authors contributed equally to the work.

Abstract: Reported herein is the development of assays for the spectrophotometric quantification of biocatalytic silicon−oxygen bond hydrolysis. Central to these assays are a series of chromogenic substrates that release highly absorbing phenoxy anions upon cleavage of the sessile bond. These substrates were tested with silicatein, an enzyme from a marine sponge that is known to catalyse the hydrolysis and condensation of silyl ethers. It was found that, of the substrates tested, *tert*-butyldimethyl(2-methyl-4-nitrophenoxy)silane provided the best assay performance, as evidenced by the highest ratio of enzyme catalysed reaction rate compared with the background (uncatalysed) reaction. These substrates were also found to be suitable for detailed enzyme kinetics measurements, as demonstrated by their use to determine the Michaelis−Menten kinetic parameters for silicatein.

Keywords: organosiloxane; enzyme; silicatein; hydrolase; colorimetric assay

check for updates

Citation: Lu, Y.; Egedeuzu, C.S.; Taylor, P.G.; Wong, L.S. Development of Improved Spectrophotometric Assays for Biocatalytic Silyl Ether Hydrolysis. *Biomolecules* **2024**, *14*, 492. https://doi.org/10.3390/biom14040492

Academic Editor: Pierre Lafite

Received: 12 March 2024
Revised: 11 April 2024
Accepted: 16 April 2024
Published: 18 April 2024

Copyright: © 2024 by the authors. Licensee MDPI, Basel, Switzerland. This article is an open access article distributed under the terms and conditions of the Creative Commons Attribution (CC BY) license (https://creativecommons.org/licenses/by/4.0/).

1. Introduction

Organosiloxanes (compounds presenting a C-Si-O chemical motif) are an important group of compounds that include silicone polymers [1] and protecting groups in multi-step organic synthesis [2,3]. However, their chemical synthetic manipulation typically requires harsh conditions and produces environmentally undesirable by-products. In efforts to improve the sustainability of silicon chemistry, researchers have been investigating enzymatic methods for the cleavage and formation of the Si-O bond [4–7]. Over the years, a host of hydrolases, including proteases, esterases, lipases and silicateins, have been investigated for their ability to catalyse the hydrolysis of Si-O bonds in a range of molecules [7–11]. Several of these enzymes have further been demonstrated to catalyse bond condensation from the corresponding silanol and alcohol though a change in the reaction conditions and hence reaction equilibrium [8,9,12].

In order to facilitate the discovery of new enzymes that can manipulate Si-O bonds and the recombinant engineering of existing enzymes, it is necessary to develop methods to detect and quantify biocatalytic Si-O bond hydrolysis. To perform such activity measurements in a convenient manner, a UV–VIS spectrophotometric assay has previously been reported using 4-nitrophenoxy silyl ethers as substrates (**1**–**3**, Scheme 1) [9,10]. Here, the hydrolysis of the Si-O bond in the substrate results in the release of a *p*-nitrophenoxy anion that absorbs strongly at approximately 400–405 nm. The presence of this chromophore may also produce a visually observable yellow colour in some cases (i.e., the assay can also be colorimetric).

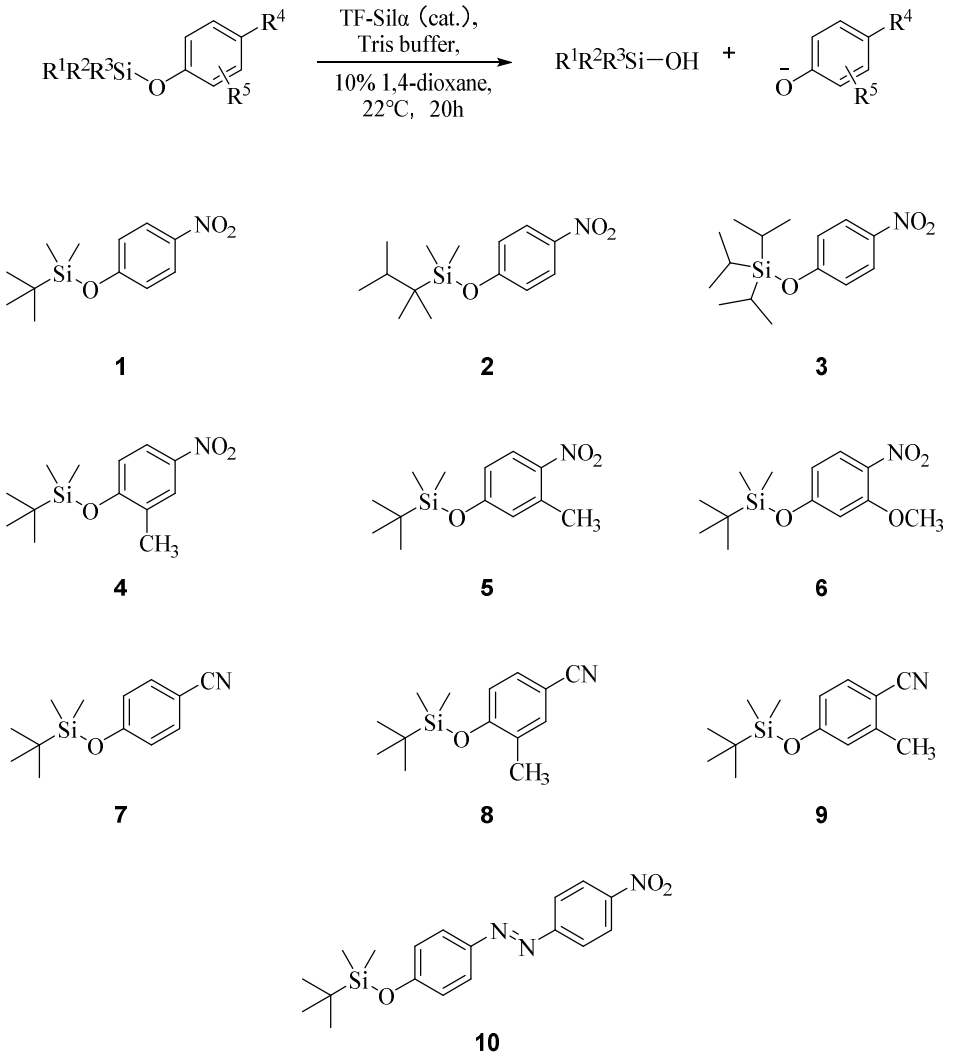

Scheme 1. Biocatalytic hydrolysis of phenoxy silyl ethers, with the structures of the various substrates shown below. R^n = various substituents as shown in the individual structures.

As an example, *tert*-butyldimethyl(4-nitrophenoxy)silane (**1**) has been used to quantify the hydrolytic activity of silicatein-α (Silα, the most common isoform of this enzyme), and subsequently to enable the determination of its Michaelis−Menten kinetic parameters [9,10]. However, it was found that this substrate generally provided a high rate of background hydrolysis, even in the absence of the enzyme under the typical assay conditions. Consequently, determining the net rate of hydrolysis (i.e., the difference between the uncatalysed and catalysed hydrolysis) tended to be less accurate at low substrate concentrations or when the enzymes exhibited low levels of activity.

Hence, the development of improved spectrophotometric assays for the quantification of Si-O bond hydrolysis is reported herein, involving the design of a set of substrates with improved stability under aqueous conditions and the tuning of the assay reaction conditions. The pro-chromogenic substrates were designed and chemically synthesised using the *tert*-butyldimethylsilyl (TBDMS) group as the silyl component. The assays were subsequently evaluated using a previously reported Silα fusion protein [10] to determine the net rates for the enzymatic reactions. The Michaelis−Menten kinetic parameters for the various substrates and this enzyme were determined as an example application.

2. Materials and Methods

2.1. Materials and Equpment

All of the solvents and reagents were of analytical grade and were purchased from either Sigma-Aldrich, Fluorochem, VWR, or Fisher Scientific. All of the buffer solutions were prepared with deionised water. Streptavidin affinity chromatography was carried out using StrepTrap HP (GE Healthcare, Amersham, UK) columns on an ÄKTA purifier chromatography system (GE Healthcare, UK). UV–VIS spectrophotometry was carried out using Synergy H1 and HT Multi-Mode Microplate Readers (BioTek Instruments, Winooski, VT, USA). Substrates **1**–**3** were synthesised according to previously reported methods [9]. The silicatein-α fusion protein production and isolation was carried out according to previously reported methods [10].

2.2. Hydrolysis Assays with TF-Silα-Strep

The assays were carried out according to previously published methods [9,10]. For experiments investigating the effect of pH, the purified TF-Silα-Strep was first dialysed in the desired buffer (50 mM Tris, 100 mM NaCl, at the desired pH) overnight. In addition, the UV−VIS absorbances for each substrate reaction were recorded at 414, 394, 398, and 294 nm, corresponding to the λ_{max} for substrates **4**, **5**, **6**, and **7**, respectively. The corresponding product phenolates were quantified with calibration curves constructed from known concentrations of each corresponding phenol. The initial rate (V_0) was obtained by a linear fit of the data from the first 30 min of the hydrolysis reaction using previously described procedures, with all of the experiments being carried out in technical triplicates [10].

2.3. General Procedure for the Synthesis of Substrates **4**–**10**

The corresponding phenol (9.98 mmol) and imidazole (19.96 mmol) were dissolved in anhydrous DMF (10 mL). *tert*-butylchlorodimethylsilane (9.98 mmol) was added to the reaction mixture and stirred at room temperature for 16 h. The reactions were all found to have reached completion after 16 h by TLC (Hexane/EtOAc, 20:1). The reaction mixture was quenched through the addition of H_2O (10 mL) and the mixture extracted with hexane (3 × 10 mL). The organic extracts were combined, dried with $MgSO_4$, filtered, and evaporated under reduced pressure. The residue was purified by silica gel chromatography to yield the desired product.

2.3.1. *tert*-Butyldimethyl(2-methyl-4-nitrophenoxy)silane, **4**

The desired product was isolated as a yellow solid (1.2 g, 45%); R_f 0.42 (Hexane/EtOAc, 20:1); ν_{max} (liquid)/cm^{-1} 2929 (C-H), 1515 (NO_2), 1280 (SiOAr), 1254 (C-O), 834 (Si-C); δ_H (400 MHz; $CDCl_3$) 8.06 (d, *J* = 2.8 Hz, 1H), 7.99 (dd, *J* = 8.9 & 2.8 Hz,1H), 6.80 (d, *J* = 8.9 Hz, 1H), 2.27 (s, 3H), 1.02 (s, 9H), 0.28 (s, 6H); δ_C (100 MHz; $CDCl_3$) 159.74 (Ar C-O), 141.29 (Ar C-N), 129.98 (Ar C-CH_3), 126.39 (Ar C-H), 122.95 (Ar C-H), 117.68 (Ar C-H), 25.42 (*t*-butyl CH_3), 18.11 (Si C-CH_3), 16.73 (Ar C-CH_3), −4.37 (Si-CH_3); *m*/*z* (ESI^+) 268 ($[M+H]^+$, 100%); HRMS calculated for $C_{13}H_{21}NO_3Si$ $[M+H]^+$: 268.1363, found: 268.1366, δ 0.9 ppm.

2.3.2. *tert*-Butyldimethyl(3-methyl-4-nitrophenoxy)silane, **5**

The desired product was isolated as a pale yellow oil (1.28 g, 49%); R_f 0.46 (Hexane/EtOAc, 20:1); ν_{max} (liquid)/cm^{-1} 2955 (C-H), 1579 and 1339 (NO_2), 1281 (SiOAr), 1251 (C-O), 824 (Si-C); δ_H (400 MHz; $CDCl_3$) 8.02 (d, *J* = 9.5 Hz, 1H), 6.73 (m, 2H), 2.59 (s, 3H), 0.99 (s, 9H), 0.25 (s, 6H); δ_C (100 MHz; $CDCl_3$) 160.46 (Ar C-O), 142.21 (Ar C-N), 137.34 (Ar C-CH_3), 127.83 (Ar C-H), 124.02 (Ar C-H), 118.35 (Ar C-H), 25.99 (*t*-butyl CH_3), 21.87 (Ar C-CH_3), 18.69 (Si C-CH_3), −3.91 (Si-CH_3); *m*/*z* (ESI^+) 267 ($[M+H]^+$, 100%); HRMS calculated for $C_{13}H_{21}NO_3Si$ $[M+H]^+$: 268.1363, found: 268.1366, δ 0.9 ppm.

2.3.3. *tert*-Butyldimethyl(3-methoxy-4-nitrophenoxy)silane, **6**

The desired product was isolated as a pale yellow solid (1.3 g, 46%); R_f 0.45 (Hexane/EtOAc, 20:1); ν_{max} (liquid)/cm^{-1} 2930 (C-H), 1581 (NO_2), 1281 (SiOAr), 1251 (C-O),

824 (Si-C); δ_H (400 MHz; $CDCl_3$) 7.91 (d, *J* = 8.9 Hz, 1H), 6.48-6.42 (m, 2H), 3.91 (s, 3H), 0.99 (s, 9H), 0.25 (s, 6H); δ_C (100 MHz; $CDCl_3$) 162.13 (Ar C-O), 156.03 (Ar C-OCH_3), 133.82 (Ar C-N), 128.56 (Ar C-H), 111.95 (Ar C-H), 105.43 (Ar C-H), 56.84 (Ar C-OCH_3), 25.96 (*t*-butyl Me), 18.69 (Si C-CH_3), −3.92 (Si-CH_3); *m*/*z* (ESI^+) 284 ($[M+H]^+$, 100%); HRMS calculated for $C_{13}H_{21}NO_4Si$ $[M+H]^+$: 284.1313, found: 284.1316, δ 1.2 ppm.

2.3.4. *tert*-Butyldimethyl(4-cyanophenoxy)silane, **7**

The desired product was given as a white solid (0.8 g, 67%); R_f 0.46 (Hexane/EtOAc, 9:1); ν_{max} (soild)/cm^{-1} 2930 (C-H), 2260 (C-N), 1281 (SiOAr), 1251 (C-O), 824 (Si-C); δ_H (400 MHz; $CDCl_3$) 7.54 (d, *J* = 8.6 Hz, 2H), 6.88 (d, *J* =8.6 Hz, 2H), 0.98 (s, 9H), 0.23 (s, 6H); δ_C (100 MHz; $CDCl_3$) 159.70 (Ar C-O), 134.01 (Ar C-H), 120.87 (Ar C-H), 119.23 (C-N), 104.64 (Ar C-CN), 25.53 (Si C-CH_3), 18.23 (Si C-CH_3), −4.40 (Si-CH_3); *m*/*z* (ESI^+) 234 ($[M+H]^+$, 100%). Data are consistent with the literature [13].

2.3.5. *tert*-Butyldimethyl(2-methyl-4-cyanophenoxy)silane, **8**

The desired product was provided as a colourless oil (115 mg, 40%); ν_{max} (liquid)/cm^{-1} 2930 (C-H), 2260 (C-N), 1281 (SiOAr), 1251 (C-O), 824 (Si-C); δ_H (400 MHz; $CDCl_3$) 7.43 (d, *J* = 2.1 Hz, 1H), 7.37 (dd, *J* = 8.3 and 2.1 Hz, 1H), 6.79 (d, *J* = 8.3 Hz, 1H) 2.21 (s, 3H), 1.01 (s, 9H), 0.25 (s, 6H). δ_C (100 MHz; $CDCl_3$) 157.82 (Ar C-O), 134.56 (Ar C-H), 131.19 (Ar C-H), 130.39 (Ar C-H), 119,27 (Ar C-H), 118.57 (C-N), 103.95 (Ar C-CN), 25.43 (Si C-CH_3), 18.08 (Si C-CH_3), 16.46, (Ar C-CH_3), −4.39 (Si-CH_3); *m*/*z* (ESI^+) 248 ($[M+H]^+$, 100%); HRMS calculated for $C_{14}H_{21}NOSi$ $[M+H]^+$: 248.1465, found: 248.1456, δ 3.5 ppm.

2.3.6. *tert*-Butyldimethyl(3-methyl-4-cyanophenoxy)silane, **9**

The desired product was provided as a colourless oil (86.76 mg, 23%); ν_{max} (liquid)/cm^{-1} 2938 (C-H), 2260 (C-N), 1281 (SiOAr), 1251 (C-O), 824 (Si-C); δ_H (400 MHz; $CDCl_3$) 7.46 (d, *J* = 8.4 Hz, 1H), 6.74 (d, *J* = 2.3 Hz, 1H), 6.70 (dd, *J* = 8.4 & 2.3 Hz 1H), 2.48 (s, 3H), 0.98 (s, 9H), 0.22 (s, 6H). δ_C (100 MHz; $CDCl_3$) 159.47 (Ar C-O), 144.12 (Ar C-H), 134.16 (Ar C-H), 121.87 (Ar C-H), 118.58 (Ar C-H), 118.09 (C-N), 105.20 (Ar C-CN), 25.54 (Si C-CH_3), 20.56 (Ar C-CH_3), 18.21 (Si C-CH_3), −4.37 (Si-CH_3); *m*/*z* (ESI^+) 248 ($[M+H]^+$, 100%); HRMS calculated for $C_{14}H_{21}NOSi$ $[M+H]^+$: 248.1465, found: 248.1456, δ 3.5 ppm.

2.3.7. (*E*)-1-(4-((*tert*-butyldimethylsilyl)oxy)phenyl)-2-(4-nitrophenyl)diazene, **10**

The desired product was provided as a red solid (178 mg, 60%); R_f 0.63 (Hexane/EtOAc, 20:1); ν_{max} (solid)/cm^{-1} 2928 (C-H), 1492 (N=N), 1339 (NO_2), 1258 (SiOAr), 854 (C-N), 781 (Si-C); δ_H (400 MHz; $CDCl_3$) 8.35 (d, *J* = 12 Hz, 2H), 7.97 (d, *J* = 8 Hz, 2H), 7.90 (d, *J* = 8 Hz, 2H), 6.97 (d, *J* = 2 Hz, 2H), 1.01 (s, 9H), 0.27 (s, 6H); δ_C (100 MHz; $CDCl_3$) 160.52 (Ar C-O), 156.49 (Ar C-N), 148.75 (Ar C-N), 147.76 (Ar C-N), 123.6 (Ar C-H), 121.15 (Ar C-H), 26.07 (Si-C-CH_3), 18.76 (Si-C-CH_3), −3.86 (Si-CH_3); *m*/*z* (ESI^+) 358 ($[M+H]^+$, 100%); HRMS calculated for $C_{18}H_{23}N_3O_3Si$ $[M+H]^+$: 358.1581, found: 358.1584, δ 0.7 ppm.

3. Results and Discussion

3.1. Design and Synthesis of Substrates

Based on the previously reported substrate **1**, a series of substrates were designed that were intended to increase the hinderance of the corresponding Si-O bond towards hydrolytic attack (steric effects), decrease the nucleofugality of the phenolate leaving group (electronic effects), or a combination of both. These included **4**–**6**, where various electron-donating substitutions were incorporated around the 4-nitrophenyl ring. The analogous 4-cyanophenoxy silyl ethers **7**–**9** were also prepared, as the cyanophenoxy moiety would be a poorer leaving group [14,15], yet still be detectable by UV–VIS spectroscopy [16,17]. In addition, substrate **10**, incorporating the azo dye 4-(4-nitrophenylazo)phenol as the chromophore, was also investigated. This dye with a *tert*-butyldiphenylsilyl group had previously been reported as a colorimetric probe for fluoride ions [18]. In this case cleavage of the Si-O bond releases the dye anion, which exhibits an absorbance at ~474 nm (in

the red region of the visible spectrum) that would be far removed from the absorbance of the substrate or any other potentially interfering molecules in an assay. In all cases, these substrates were synthesised by the silylation of the corresponding phenols and silyl chloride under basic conditions, with moderate yields between 45–70%.

3.2. pH Optimisation of Assay

One likely reason for the relatively poor difference in rates between the enzymatic and uncatalysed reaction from the originally reported assay method [10] was the relatively high pH in which they were carried out. Thus, the effect of pH on the hydrolysis of **1** was first investigated. Silα, fused with the trigger factor at the *N*-terminal and a Strep-tag II affinity tag at the *C*-terminal (henceforth referred to as TF-Silα-Strep) was used as the model enzyme. The data from the enzymatic reactions were then compared to non-enzymatic hydrolysis, where the enzyme had been omitted from the reaction mixtures. As expected, it was found that the rate of non-enzymatic hydrolysis increased with pH (Figure 1A). A similar trend was observed with the enzymatic reaction, but once the net rate was calculated, the enzyme was found to exhibit a good activity between 6.5–8.5 (Figure 1B), with an optimal pH of 8.5. This value is consistent with the optimal pH range for serine proteases such as chymotrypsin and trypsin, as well as the alkaline proteases [9,19,20].

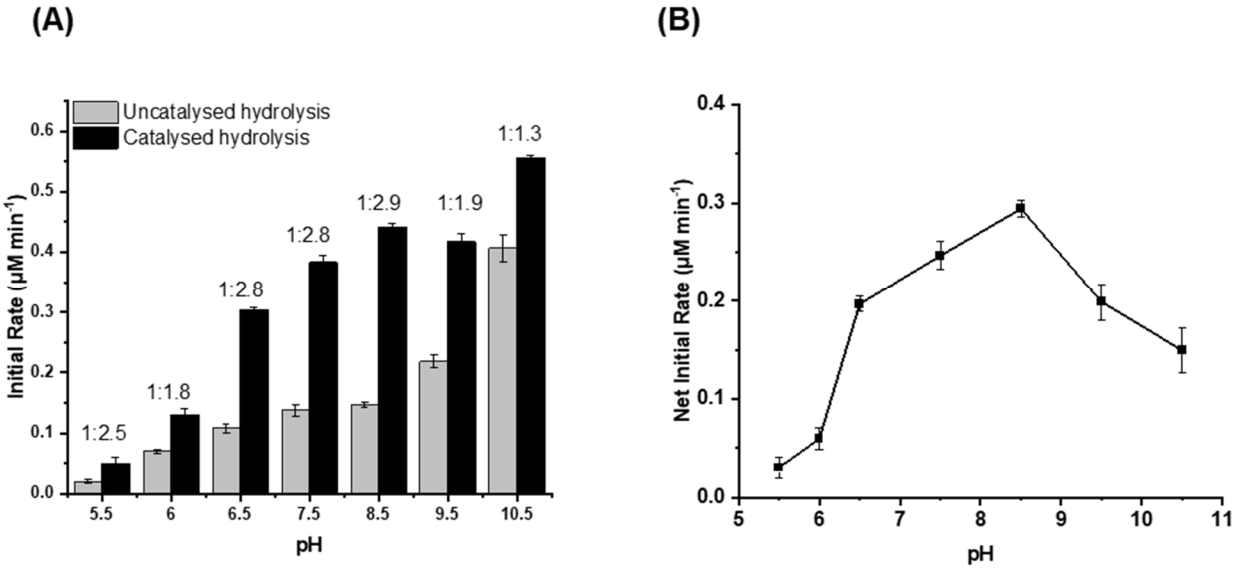

Figure 1. Plots of initial rate of hydrolysis of **1** against pH for (**A**) reactions that are uncatalysed (enzyme omitted) and catalysed (where the enzyme was present) and (**B**) the net enzymatic rate of hydrolysis. The net rate is calculated by subtracting the rate of the uncatalysed reaction from the reactions where the enzyme is present. The ratios of the catalysed to uncatalysed reactions are provided above each column pair. The error bars represent the standard error from triplicate experiments. Enzymatic reactions are carried out with 6.7 μM TF-Silα-Strep, 50 μM **1**, 10% *v*/*v* 1,4-dioxane, 50 mM Tris buffer at the appropriate pH and 100 mM NaCl.

3.3. Substrate Screening

The hydrolysis of the new substrates **4**–**10** was subsequently tested in a similar manner at pH 8.5. However, during these experiments, it was found that the azobenzene-derived substrate **10** and methyl substituted cyanophenol substrates **8** and **9** were essentially insoluble in the reaction mixture, even though it already contained 10% *v*/*v* 1,4-dioxane as a co-solvent. DMSO was also tested as an alternative biocompatible solvent (at the same concentration), but was found to be ineffective, and these substrates were therefore excluded from further investigation. Of the remaining substrates, the reaction conversions were quantified by UV–VIS spectrophotometry (Figure S1 in SI), and their corresponding initial rates were calculated (Figure 2, Table S1 in SI).

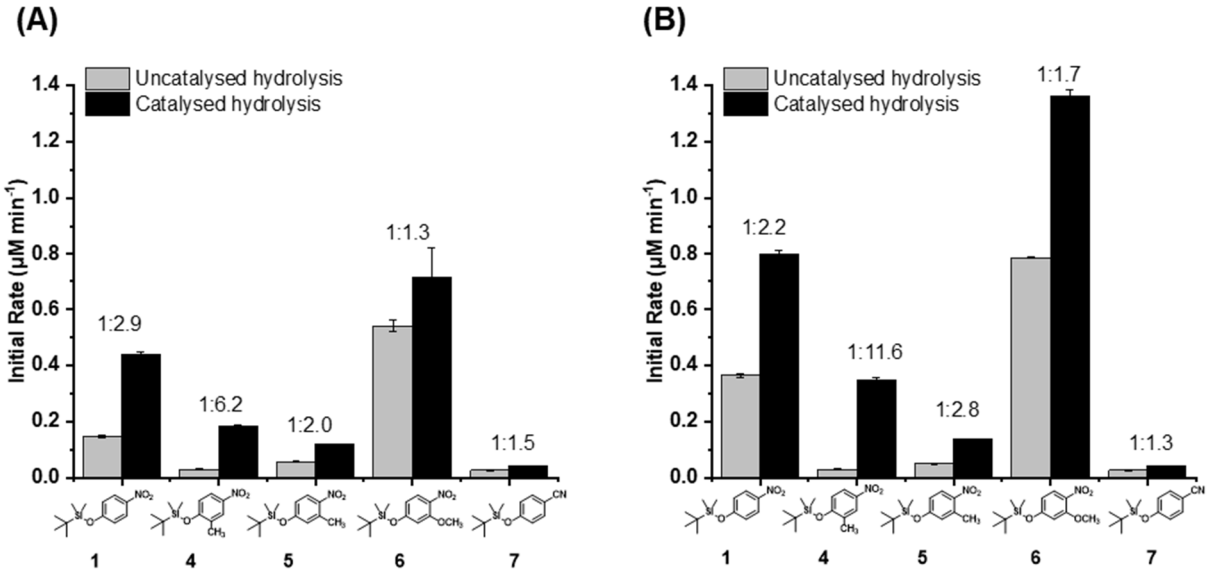

Figure 2. The initial rates of enzyme catalysed and background (non-enzymatic) hydrolysis of the substrates **1**, **4**–**7** (at either 50 or 100 μM of substrate; (**A**) and (**B**), respectively). The ratios of the catalysed to uncatalysed reaction are provided above each column pair. The error bars represent the standard error from triplicate experiments. Enzymatic reactions were carried out with 6.7 μM TF-Silα-Strep, 50 μM or 100 μM substrate, 10% *v*/*v* 1,4-dioxane, 50 mM Tris buffer at pH 8.5 and 100 mM NaCl.

In the assays employing the 50 μM substrate (the same concentration as used in previous work), the ratio of enzymatic to non-enzymatic rates (Figure 2A) showed that **4** provided the greatest differentiation between the enzymatic reaction and the uncatalysed hydrolysis. Here, a ratio of 6.2 between the two rates was achieved, although in both (enzymatic and uncatalysed) the absolute rates were lower compared with the parent substrate **1**. The slower rates with the 2-methyl substituted (i.e., *ortho* relative to the scissile Si-O bond) **4** were likely due to the mildly electron-donating effect of this substituent, as well as steric blocking. Significantly, the uncatalysed reaction appeared to be retarded to a greater degree than the enzymatic reaction, although the reason was unclear. The 3-methyl substrate **5** provided uniformly lower rates for the enzymatic and non-enzymatic reactions compared with the parent **1**. This result is consistent with the fact that the methyl group prevents the neighbouring nitro group from being coplanar with the ring, thereby making the nitrophenoxide a poorer leaving group.

In contrast, the methoxy-substituted **6** provided the highest rates for both reactions, so clearly the inductive electron-withdrawing effects were more important than any mesomeric stabilisation of the putative-leaving group. The 4-cyanophenoxy substrate **7** was anticipated to provide much lower rates of reaction compared with **1,** given the cyano group's less negative Hammett σ constant (−0.56) compared with the nitro group (−0.71) [21], and this was indeed observed in the experimental results. Although the addition of the enzyme did provide a higher rate of hydrolysis for substrate **7** compared with when the enzyme was omitted, the difference was the smallest among the tested substrates, suggesting that **7** was less well accepted by the enzyme.

To assess the effect of the substrate concentration, which may affect enzyme occupancy (see below), the assay was then carried out with 100 μM of substrate (Figure 2B, Figure S1 and Table S1 in SI). As expected, the absolute rates were found to be higher in all cases due to the increase in substrate concentration. However, it was also found that the ratio of enzymatic to uncatalysed reactions were improved for substrates **4** and **5**. In the case of **4**, a dramatic increase to a ratio was observed with the enzymatic reaction being nearly 12-fold greater than the uncatalysed reaction. These results suggest that the substrate binding to

the enzyme is relatively weak and at the lower substrate concentration, enzyme occupancy (and hence enzyme-catalysed turnover) was suboptimal.

Overall, the ratios of enzymatic to background reaction rates for substrates **5**, **6**, and **7** were inferior to the original substrate **1**. Only substrate **4** produced an improved result that could be translated to a superior signal-to-noise ratio in the subsequent Michaelis–Menten kinetics measurements (see below).

3.4. Kinetic Analysis of TF-Silα-Strep on Silyl Ether Hydrolysis

To demonstrate the utility of the new substrates for quantitative enzyme kinetics analyses, the molecules **4** and **5** that displayed the two best rate ratios were then applied in enzyme assays to determine their Michaelis–Menten kinetic parameters with respect to TF-Silα-Strep (using the net rates of reaction, as previously reported). For consistency, the kinetic parameters for the previously reported substrates **1**–**3** were also determined. The results obtained from the Michaelis–Menten plots (Table 1, Figures S2 and S3 in SI) showed that all of the substrates had K_M in the μM range, which were consistent with the results previously reported for **1** [10]. The 2-methyl substrate **4** exhibited a K_M of 72.5 μM, which was substantially higher than the other substrates (i.e., weaker binding or fewer productive binding events). This result is consistent with the substrate screening experiments above, whereby the use of 100 μM of substrate (i.e., above the K_M) provided an improvement in the ratio of catalysed to uncatalysed hydrolysis.

Table 1. Table of Michaelis−Menten constants determined for TF-Silα-Step against substrates **1**–**5**. The data and plots from which these values are derived are provided in Figures S2 and S3 in the SI. Assays are performed in 10% v/v 1,4-dioxane, 50 mM Tris, and100 mM NaCl, pH 8.5.

Substrate	K_M (μM)	k_{cat} (min^{-1})
1	44.4 ± 11.9	0.0858 ± 0.0102
2	24.1 ± 5.00	0.0136 ± 0.0010
3	20.4 ± 8.13	0.0023 ± 0.0003
4	72.5 ± 15.3	0.0577 ± 0.0101
5	34.6 ± 4.11	0.0247 ± 0.0013

In comparing the k_{cat} of the TBDMS-bearing substrates, the unsubstituted **1** provided the highest rate constant, which was unsurprising as the introduction of the methyl groups in **4** and **5** were intended to reduce their susceptibility to hydrolysis. In comparing **1**–**3**, increasing steric bulk of the silyl groups reduced k_{cat} due to the reduction in accessibility of the Si–O bond. This steric bulk in **2** and **3** had a much greater effect than the methylations in **4** and **5**.

4. Conclusions

In summary, this study reports the development of chromogenic substrates that are applicable for the spectrophotometric quantification of biocatalytic Si-O bond hydrolysis. A series of molecules bearing a sessile Si-O bond attached to a chromophore were synthesised, characterised, and, where possible, their rates of hydrolysis were measured under conditions that are suitable for the enzymatic assay. Here, the ratio of the initial rates of the enzymatic and non-enzymatic reactions was used as the key criterion for determining the optimal substrate and reaction conditions.

It was found that for the model silicatein enzyme, *tert*-butyldimethyl(2-methyl-4-nitrophenoxy)silane (**4**) displayed the best rate ratio of enzyme-catalysed to uncatalysed reactions, albeit with lower absolute rates. This finding underscores the potential of employing tailored spectrophotometric substrates to provide a better signal-to-noise ratio for improved accuracy. However, the subsequent Michaelis−Menten kinetics analysis demonstrated that care should be taken in the selection of substrates so they are matched to the binding affinity of the enzyme of interest. Nevertheless, from a practical perspective

the use of lower quantities of substrate to conserve reagents may still find utility as a qualitative assay.

Potential avenues for future work include an exploration of substrate diversity to include alternative chromophores and the investigation of fluorogenic assays for broader analytical applications and further improved sensitivity. In terms of wider applications, the molecules reported here could also be used as part of an assay for the detection of fluoride ions [18].

Supplementary Materials: The following supporting information can be downloaded at: https://www.mdpi.com/article/10.3390/biom14040492/s1. Figure S1: Graph of concentration of silanols produced showing enzymatic and non-enzymatic (background) hydrolysis measured at the λ_{max} of their corresponding 4-nitrophenolate ions after 300 min. Table S1: Comparative analysis of the background hydrolysis vs enzymatic hydrolysis showing the initial rates and fold increase of enzyme on silyl ethers. Figure S2: Graph of net concentration of corresponding silanols produced from silyl ether substrates measured by UV−VIS absorbance at λ_{max} of their respective 4-nitrophenolate anions. Figure S3: Graph of best fit Michaelis–Menten curves for the hydrolysis of silyl ether substrates by TF-Silα-Strep against a range of substrate concentrations. Figure S4: Calibration graph of UV−VIS absorption against concentration of (**A**) 4-nitrophenol for **1**, (**B**) 2-methyl-4-nitrophenol for **4**, (**C**) 3-methyl-4-nitrophenol for **5**, (**D**) 3-methoxy-4-nitrophenol for **6**, and (**E**) 4-cyanophenol for **7**. Figures S5–S14: Calibrated NMR spectra for substrates **1**–**10** showing ^{1}H (**top**) and ^{13}C (**bottom**) chemical shifts. Figure S15: ESI+ mass spectra of substrate **1**–**10**.

Author Contributions: Conceptualisation, L.S.W.; methodology, Y.L. and C.S.E.; validation, Y.L. and C.S.E.; formal analysis, Y.L., C.S.E. and L.S.W.; investigation, Y.L. and C.S.E.; resources; data curation, Y.L.; writing—original draft preparation, Y.L.; writing—review and editing, Y.L., C.S.E., P.G.T. and L.S.W.; visualisation, Y.L.; supervision, L.S.W.; project administration, L.S.W.; funding acquisition, Y.L., P.G.T. and L.S.W. All authors have read and agreed to the published version of the manuscript.

Funding: This research was supported by the UK Engineering and Physical Sciences Research Council under grant EP/S013539/1, and equipment purchased under grant EP/K011685/1. C.S.E. thanks the Tertiary Education Trust Fund of Nigeria for a graduate scholarship.

Data Availability Statement: Numerical data are available from the authors upon request.

Conflicts of Interest: The authors declare no conflicts of interest. The funders had no role in the design of the study; in the collection, analyses, or interpretation of data; in the writing of the manuscript; or in the decision to publish the results.

References

1. Andriot, M.; DeGroot, J.V.; Meeks, R.; Wolf, A.T.; Leadley, S.; Garaud, J.L.; Gubbels, F.; Lecomte, J.P.; Lenoble, B.; Stassen, S.; et al. Silicones in Industrial Applications. In *Inorganic Polymers*; Nova Science Pub Inc.: Hauppauge, NY, USA, 2007; pp. 61–161.
2. Corey, E.J.; Venkateswarlu, A. Protection of Hydroxyl Groups as Tert-Butyldimethylsilyl Derivatives. *J. Am. Chem. Soc.* **1972**, *94*, 6190–6191. [CrossRef]
3. D'Sa, B.A.; McLeod, D.; Verkade, J.G. Nonionic Superbase-Catalyzed Silylation of Alcohols. *J. Org. Chem.* **1997**, *62*, 5057–5061. [CrossRef]
4. Frampton, M.B.; Zelisko, P.M. Biocatalysis in Silicon Chemistry. *Chem. Asian J.* **2017**, *12*, 1153–1167. [CrossRef]
5. Sarai, N.S.; Levin, B.J.; Roberts, J.M.; Katsoulis, D.E.; Arnold, F.H. Biocatalytic Transformations of Silicon—The Other Group 14 Element. *ACS Cent. Sci.* **2021**, *7*, 944–953. [CrossRef] [PubMed]
6. Bassindale, A.R.; Brandstadt, K.F.; Lane, T.H.; Taylor, P.G. Enzyme-Catalysed Siloxane Bond Formation. *J. Inorg. Biochem.* **2003**, *96*, 401–406. [CrossRef] [PubMed]
7. Frampton, M.B.; Simionescu, R.; Dudding, T.; Zelisko, P.M. The Enzymatic Cleavage of Si–O Bonds: A Kinetic Analysis of the Biocatalyzed Hydrolysis of Phenyltrimethoxysilane. *J. Mol. Catal. B Enzym.* **2010**, *66*, 105–112. [CrossRef]
8. Abbate, V.; Bassindale, A.R.; Brandstadt, K.F.; Taylor, P.G. A Large Scale Enzyme Screen in the Search for New Methods of Silicon–Oxygen Bond Formation. *J. Inorg. Biochem.* **2011**, *105*, 268–275. [CrossRef] [PubMed]
9. Dakhili, S.Y.T.; Caslin, S.A.; Faponle, A.S.; Quayle, P.; De Visser, S.P.; Wong, L.S. Recombinant Silicateins as Model Biocatalysts in Organosiloxane Chemistry. *Proc. Natl. Acad. Sci. USA* **2017**, *114*, E5285–E5291. [CrossRef]
10. Sparkes, E.I.; Kettles, R.A.; Egedeuzu, C.S.; Stephenson, N.L.; Caslin, S.A.; Dakhili, S.Y.T.; Wong, L.S. Improved Production and Biophysical Analysis of Recombinant Silicatein-α. *Biomolecules* **2020**, *10*, 1209. [CrossRef] [PubMed]
11. Brondani, P.; Mittersteiner, M.; Voigt, M.; Klinkowski, B.; Riva Scharf, D.; de Jesus, P. Synthetic Versatility of Lipases: Application for Si–O Bond Formation and Cleavage. *Synthesis* **2019**, *51*, 477–485. [CrossRef]

12. Sparkes, E.I.; Egedeuzu, C.S.; Lias, B.; Sung, R.; Caslin, S.A.; Tabatabaei Dakhili, S.Y.; Taylor, P.G.; Quayle, P.; Wong, L.S. Biocatalytic Silylation: The Condensation of Phenols and Alcohols with Triethylsilanol. *Catalysts* **2021**, *11*, 879. [CrossRef]
13. Dorval, C.; Tricoire, M.; Begouin, J.-M.; Gandon, V.; Gosmini, C. Cobalt-Catalyzed C(Sp 2)–CN Bond Activation: Cross-Electrophile Coupling for Biaryl Formation and Mechanistic Insight. *ACS Catal.* **2020**, *10*, 12819–12827. [CrossRef]
14. Carvalho, E.; Francisco, A.P.; Iley, J.; Rosa, E. The Mechanism of Hydrolysis of Aryl Ether Derivatives Of3-Hydroxymethyltriazenes. *Eur. J. Org. Chem.* **2005**, *2005*, 2056–2063. [CrossRef]
15. Onyido, I.; Swierczek, K.; Purcell, J.; Hengge, A.C. A Concerted Mechanism for the Transfer of the Thiophosphinoyl Group from Aryl Dimethylphosphinothioate Esters to Oxyanionic Nucleophiles in Aqueous Solution. *J. Am. Chem. Soc.* **2005**, *127*, 7703–7711. [CrossRef] [PubMed]
16. Fedorova, A.A.; Sokolova, I.V. Development of Method for Destruction of 4-Cyanophenol Using Photolysis and Activated Oxidative Processes. *J. Appl. Spectrosc.* **2023**, *90*, 825–829. [CrossRef]
17. Yu, Z.-C.; Lu, Y.; Zhao, J.; Dai, J.-J.; Chen, G.-R.; Shan, P.-H.; Redshaw, C.; Tao, Z.; Xiao, X. A Study of the Supramolecular Assembly Formed by Cucurbit[7]Uril and 4-Cyanophenol. *J. Mol. Struct.* **2023**, *1278*, 134969. [CrossRef]
18. Cheng, X.; Li, S.; Xu, G.; Li, C.; Qin, J.; Li, Z. A Reaction-Based Colorimetric Fluoride Probe: Rapid "Naked-Eye" Detection and Large Absorption Shift. *Chempluschem* **2012**, *77*, 908–913. [CrossRef]
19. Kirschke, H.; Langer, J.; Wiederanders, B.; Ansorge, S.; Bohley, P.; Cathepsin, L. A new proteinase from rat-liver lysosomes. *Eur. J. Biochem.* **1977**, *74*, 293–301. [CrossRef] [PubMed]
20. Sanatan, P.T.; Lomate, P.R.; Giri, A.P.; Hivrale, V.K. Characterization of a Chemostable Serine Alkaline Protease from Periplaneta Americana. *BMC Biochem.* **2013**, *14*, 32. [CrossRef] [PubMed]
21. Hansch, C.; Leo, A.; Taft, R.W. A Survey of Hammett Substituent Constants and Resonance and Field Parameters. *Chem. Rev.* **1991**, *91*, 165–195. [CrossRef]

Disclaimer/Publisher's Note: The statements, opinions and data contained in all publications are solely those of the individual author(s) and contributor(s) and not of MDPI and/or the editor(s). MDPI and/or the editor(s) disclaim responsibility for any injury to people or property resulting from any ideas, methods, instructions or products referred to in the content.